CARDIOVASCULAR DISEASE

Reloadable multidrug capturing delivery system for targeted ischemic disease treatment

Jasmine P. J. Wu,[1] Bill Cheng,[1] Steve R. Roffler,[1,2]* David J. Lundy,[1] Christopher Y. T. Yen,[1] Peilin Chen,[3] James J. Lai,[4] Suzie H. Pun,[4] Patrick S. Stayton,[4] Patrick C. H. Hsieh[1,4,5]*

Human clinical trials of protein therapy for ischemic diseases have shown disappointing outcomes so far, mainly because of the poor circulatory half-life of growth factors in circulation and their low uptake and retention by the targeted injury site. The attachment of polyethylene glycol (PEG) extends the circulatory half-lives of protein drugs but reduces their extravasation and retention at the target site. To address this issue, we have developed a drug capture system using a mixture of hyaluronic acid (HA) hydrogel and anti-PEG immunoglobulin M antibodies, which, when injected at a target body site, can capture and retain a variety of systemically injected PEGylated therapeutics at that site. Furthermore, repeated systemic injections permit "reloading" of the capture depot, allowing the use of complex multistage therapies. This study demonstrates this capture system in both murine and porcine models of critical limb ischemia. The results show that the reloadable HA/anti-PEG system has the potential to be clinically applied to patients with ischemic diseases, who require sequential administration of protein drugs for optimal outcomes.

INTRODUCTION

Successful tissue regeneration after ischemic incidents, such as myocardial infarction and critical limb ischemia, remains a major clinical challenge. It is widely accepted that neovascularization in the ischemic area is the key to the overall success of the regenerative process (*1*, *2*). However, although individual proangiogenic factors have been shown to stimulate neovascularization in various animal models of ischemia, human clinical trials using single-protein therapies have shown disappointing results. Instead, it has become clear that clinical success requires multiple proangiogenic proteins, such as insulin-like growth factor 1 (IGF-1), granulocyte colony-stimulating factors (G-CSFs), vascular endothelial growth factors, and fibroblast growth factors, delivered at appropriate time points (*2*, *3*)—much like the natural process of vascular regeneration after ischemic injury.

Although concomitant administrations of proangiogenic factors can stimulate vascularization in ischemic areas in rodent models (*4*), recent studies have indicated that sequential administration of growth factors often produces better therapeutic outcomes (*5*). It is further recognized that the synergistic effects of most proangiogenic proteins are time-dependent (*6*). For example, a study using minocycline and candesartan in a rat model of ischemic stroke reported that the overall therapeutic effect was reduced when the drugs were administered concomitantly. It was later revealed that minocycline, an antioxidant, can inhibit the proangiogenic activity of candesartan (*7*). Thus, by sequential administration of candesartan followed by minocycline, the synergistic drug effect was recovered (*8*).

Although sequential drug therapy has been suitably demonstrated in various animal models, the clinical translations of these therapies to human patients have been modest at best (*9*). One key challenge is the short half-life of exogenous, unmodified peptide growth factors in the blood stream and their poor uptake and retention by the injured site. One common approach is to increase the circulating half-life of drugs through the attachment of polyethylene glycol (PEG) chains (*10*, *11*). However, if these PEGylated drugs are poorly retained at the desired target site, the prolonged presence of these drugs in circulation may result in generation of antibodies against the PEG moiety (*12*–*14*).

Because ischemic tissues only display a modest, short-lived enhanced permeability and retention (EPR) effect, we sought to develop a system that could enhance the retention of PEGylated proteins at a chosen ischemic target site. Here, we present a drug capture system that, when injected at the ischemic area, can capture and retain PEG-modified compounds at that site, thus improving their therapeutic efficacy. This capture system consists of high-affinity anti-PEG immunoglobulin M (IgM) antibodies, AGP4, which are injected and retained at the ischemic border zone suspended in a biocompatible hyaluronic acid (HA) hydrogel. This capture system was then used to improve the therapeutic efficacy of PEG-modified protein growth factor–based therapy for limb ischemia in both rodent and porcine models.

RESULTS

AGP4 antibody depots capture and retain PEGylated compounds

The binding affinity of anti-PEG antibodies (AGP4) to two commercially available nanosized PEGylated compounds, PEG-Qd800 and Lipo-Dox, was confirmed in vitro by sandwich enzyme-linked immunosorbent assay (ELISA) (fig. S1). For in vivo tracking experiments, PEG-Qd800 was selected as a model drug to be delivered to Alexa Fluor 647–labeled AGP4 depots. The fluorescence signals of these fluorophores were shown to be nonoverlapping, using the in vivo imaging system (IVIS) (fig. S2).

HA is a biodegradable material approved by the U.S. Food and Drug Administration (FDA) for use in local injections (*15*, *16*), which also promotes neovascularization in ischemic tissue (*17*). To demonstrate the ability of the capture system to retain PEG-modified compounds, fluorescence-labeled AGP4 antibody mixed with 1% (w/v) HA (HA/AGP4) was subcutaneously injected at three different locations in mice, followed 10 min later by intravenous administration of PEG-Qd800s (Fig. 1A). The results show that AGP4 was retained at the three injection sites by the hydrogel and that systemically injected PEG-Qd800s were

[1]Institute of Biomedical Sciences, Academia Sinica, Taipei 115, Taiwan. [2]Graduate Institute of Medicine, College of Medicine, Kaohsiung Medical University, Kaohsiung 80708, Taiwan. [3]Research Center for Applied Sciences, Academia Sinica, Taipei 115, Taiwan. [4]Department of Bioengineering, University of Washington, Seattle, WA 98195, USA. [5]Institute of Medical Genomics and Proteomics and Department of Surgery, National Taiwan University and Hospital, Taipei 100, Taiwan.
*Corresponding author. Email: phsieh@ibms. sinica.edu.tw (P.C.H.H.); sroff@ibms. sinica.edu.tw (S.R.R.)

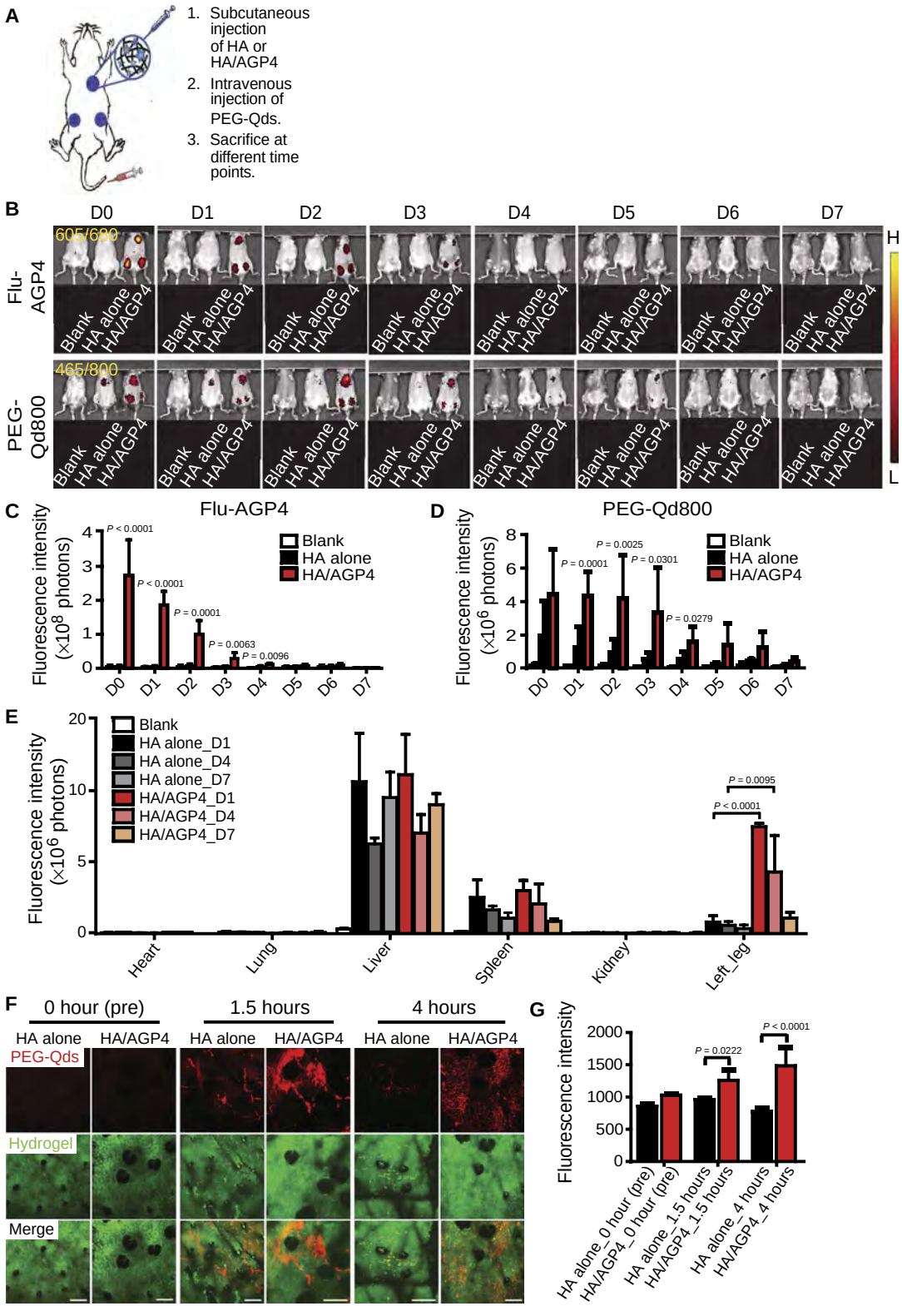

Fig. 1. In vivo demonstration of HA/anti-PEG capture system. (**A**) Schematic diagram showing the experimental design. (**B**) Representative IVIS images of mice after a single subcutaneous injection of fluorescence-labeled anti-PEG (Flu-AGP4) and intravenous administration of PEG-Qd800s. Flu-AGP4 was visualized at 605/680 nm, and PEG-Qd800s were visualized at 465/800 nm. HA alone was used as a control. D, day. (**C**) Quantification of Flu-AGP4 signal over 7 days. (**D**) Quantification of PEG-Qd800 signal over 7 days. (**E**) Biodistribution of systemically injected PEG-Qd800s at days 1, 4, and 7. (**F**) Intravital imaging of mouse ear with fluorescein isothiocyanate (FITC)–labeled HA hydrogel before and at 1.5 and 4 hours after systemic PEG-Qd800 administration. Scale bars, 50 μm. (**G**) Quantification of PEG-Qd800 fluorescence intensity. Data are means ± SD. Blank, $n = 3$; HA alone, $n = 6$; HA/AGP4, $n = 6$.

captured and retained at those same three HA/AGP4 injection sites, remaining measurable until day 6 (Fig. 1B). Some passive uptake of quantum dots was noted in the HA-alone group; however, this was only temporary. The fluorescence signals of AGP4 and PEG-Qd800s were quantified and analyzed, as shown in Fig. 1 (C and D, respectively), and an assessment of PEG-Qd800 systemic biodistribution on the first, fourth, and seventh days revealed significantly higher PEG-Qd800 detections on the first ($P < 0.0001$, $n = 6$) and fourth ($P = 0.0095$, $n = 6$) days with HA/AGP4 injection compared to HA alone (Fig. 1E).

Intravital multiphoton microscopy was also used to confirm the extravasation of PEG-Qds (fig. S3 and movies S1 to S4). Imaging of the HA/AGP4 injection site revealed that a significant amount of PEG-Qd655s (red) entered the injection site (green) from the capillaries (Fig. 1, F and G) during the first 1.5 hours after intravenous injection ($P = 0.0222$, $n = 3$) and further increased at 4 hours ($P < 0.0001$, $n = 3$).

PEG-Qd800s administered on different days are retained by the same HA/AGP4 system

We next sought to determine whether multiple systemic injections of PEGylated compounds could increase the amount captured at an intramuscular target site. As summarized in Fig. 2A, HA/AGP4 was first injected into the left leg muscle of mice, followed by three intravenous injections of PEG-Qd800 into the tail vein on days 1, 2, and 3. After one injection of PEG-Qd800s, the results were similar to those shown in Fig. 1, as expected. However, the mice receiving three PEG-Qd800 injections (Fig. 2B, bottom panel, right mouse) showed significantly greater PEG-Qd800 fluorescence intensity at the HA/AGP4 injection site compared to the other two groups (day 2, $P < 0.0001$; day 3, $P = 0.0002$; day 7, $P = 0.0076$; $n = 6$), and the PEG-Qd800 signal remained visible until day 7, compared to day 3, after a single injection (Fig. 2C). The results demonstrate that the capture site was successfully "reloaded" with PEG-Qd800s, thus allowing repeated systemic doses to be delivered to the target area.

Ex vivo analysis of the fluorescence signal in the leg muscles confirmed the enhanced retention of PEG-Qd800s in the HA/AGP4-injected left leg muscle compared to the control leg (Fig. 2D, second row from the top). Fluorescence intensity was quantified, as shown in Fig. 2E. Although more PEG-Qd800s were retained in the liver after three injections compared to one injection, the degree of increase in the AGP4-injected leg muscle was much greater. Immunofluorescence staining analysis (Fig. 2, F and G) supports the IVIS data, showing greater retention of PEG-Qd800s in HA/AGP4-injected tissues after one quantum dot administration and even greater retention after three quantum dot administrations ($P = 0.0007$, $n = 6$).

The anti-PEG drug capture system was evaluated for treating hind limb ischemia

Next, we sought to apply this drug capture system to develop a therapeutic regimen using multiple PEGylated growth factors. A hind limb ischemia (HLI) model was used to induce injury in one leg of male FVB mice, and HA/AGP4, HA alone, or phosphate-buffered saline (PBS) was injected into four sites surrounding the ischemic area—one in the calf and three in the thigh. IGF-1 has been previously shown to protect ischemic tissues from damage (*18*, *19*). Therefore, three intravenous injections of PEG-modified IGF-1 were given every 8 hours, as shown in Fig. 3A. The laser Doppler blood flow measurements and gross morphology shown in Fig. 3B demonstrate a reduction in tissue damage in mice receiving HA/AGP4 and PEG–IGF-1 compared to mice receiving intramuscular PBS or HA alone. Terminal deoxynucleotidyl transferase–mediated deoxyuridine triphosphate nick end labeling (TUNEL) analysis of the ischemic region (Fig. 3, C and D) revealed significantly fewer apoptotic cells (HA/anti-PEG + PBS versus HA/anti-PEG + PEG–IGF-1, $P < 0.0001$; HA alone + PEG–IGF-1 versus HA/anti-PEG + PEG–IGF-1, $P = 0.0002$; $n = 6$), and Fig. 3E shows increased human IGF-1 present at the HA/AGP4 injection site compared to controls.

G-CSF increases production and recruitment of hematopoietic and endothelial progenitor cells to injury sites (*20*–*23*). Therefore, using the same strategy previously outlined, we injected three doses of PEG-modified G-CSF into mice with HLI at 24-hour intervals, as shown in Fig. 4A. Figure 4B shows improved tissue morphology after 4 days in mice receiving intramuscular HA/AGP4 and intravenous PEG–G-CSF. Staining the ischemia-injured area for $CD34^+/CD133^+$ cells revealed a significant increase in recruitment of hematopoietic and endothelial progenitor cells in HA/AGP4, PEG–G-CSF–treated animals compared to controls (versus HA alone + PEG–G-CSF, $P = 0.0003$; versus HA/anti-PEG + PBS, $P < 0.0001$; $n = 6$), as shown in Fig. 4 (C and D). Figure 4E reveals increased human G-CSF present at the HA/AGP4 injection site compared to controls.

On the basis of these results, we investigated the therapeutic effect of sequential delivery of both PEG–IGF-1 and PEG–G-CSF to the HA/AGP4 injection site over a longer treatment course after HLI injury. The dosing scheme is shown in Fig. 5A. Because the role of IGF-1 is to protect cells from ischemia-induced apoptosis, PEG–IGF-1 was administered in three doses at 8-hour intervals immediately after HLI injury. However, G-CSF acts over a longer time period to facilitate cell recruitment and blood vessel generation, and therefore, PEG–G-CSF was administered at 24-hour intervals for 3 days after HLI. This dosing regimen takes advantage of the reloadable nature of the HA/AGP4 drug capture system to deliver repeated doses of PEGylated compounds to the target site.

The results show improvements in therapeutic outcome after 28 days for mice receiving the HA/AGP4 capture system at the ischemic injury site. Compared to the HA alone and PBS control groups, the HA/AGP4 group displayed almost complete recovery of blood flow as early as day 14, and its blood flow was comparable to the sham group at day 28 (Fig. 5, B and C). Although the HA-alone and PBS control groups also displayed improvements in blood flow throughout the 28-day period, these mice showed signs of calf muscle atrophy as early as day 7 and toe necrosis at day 21. Closer examination reveals that mice receiving HA/AGP4 and the combined growth factor treatment have clearly separated, elongated toes with preserved toe nails, whereas mice receiving HA alone have shorter, stubby toes with loss of toenails and smaller paw pads. These changes are reflected in the clinical scores presented in Fig. 5D, which show a clear improvement in the HA/AGP4 group compared to controls, as shown in table S1. Examination of representative tissue sections encompassing the ischemic site (Fig. 5, E and F) revealed a significantly larger number of capillaries in the ischemic tissue of mice receiving HA/AGP4 and the combined growth factor therapy (versus HA/combined therapy, $P = 0.0042$; versus HA/AGP4 + PBS, $P < 0.0001$; $n = 8$ to 12). It is clear from these results that, although systemic administration of IGF-1 and G-CSF was partially effective in promoting recovery from limb ischemia, the addition of the HA/AGP4 capture system markedly improved the efficacy of this therapy.

HA/AGP4 administration appears safe and does not cause immunogenicity in immunocompetent mice

To assess the potential immunogenicity or toxicity of HA/AGP4, FVB mice were injected with HA/AGP4, as described previously. A

complement C3 ELISA showed no significant complement activation in either plasma or muscle tissue 3 days after intramuscular injection of HA/AGP4 compared to HA/IgM or HA alone (fig. S4). Furthermore, there were no changes in total circulating white blood cell count or white cell differential after HA/AGP4 administration (table S2). Serum chemistry analysis showed no adverse changes in either liver or kidney

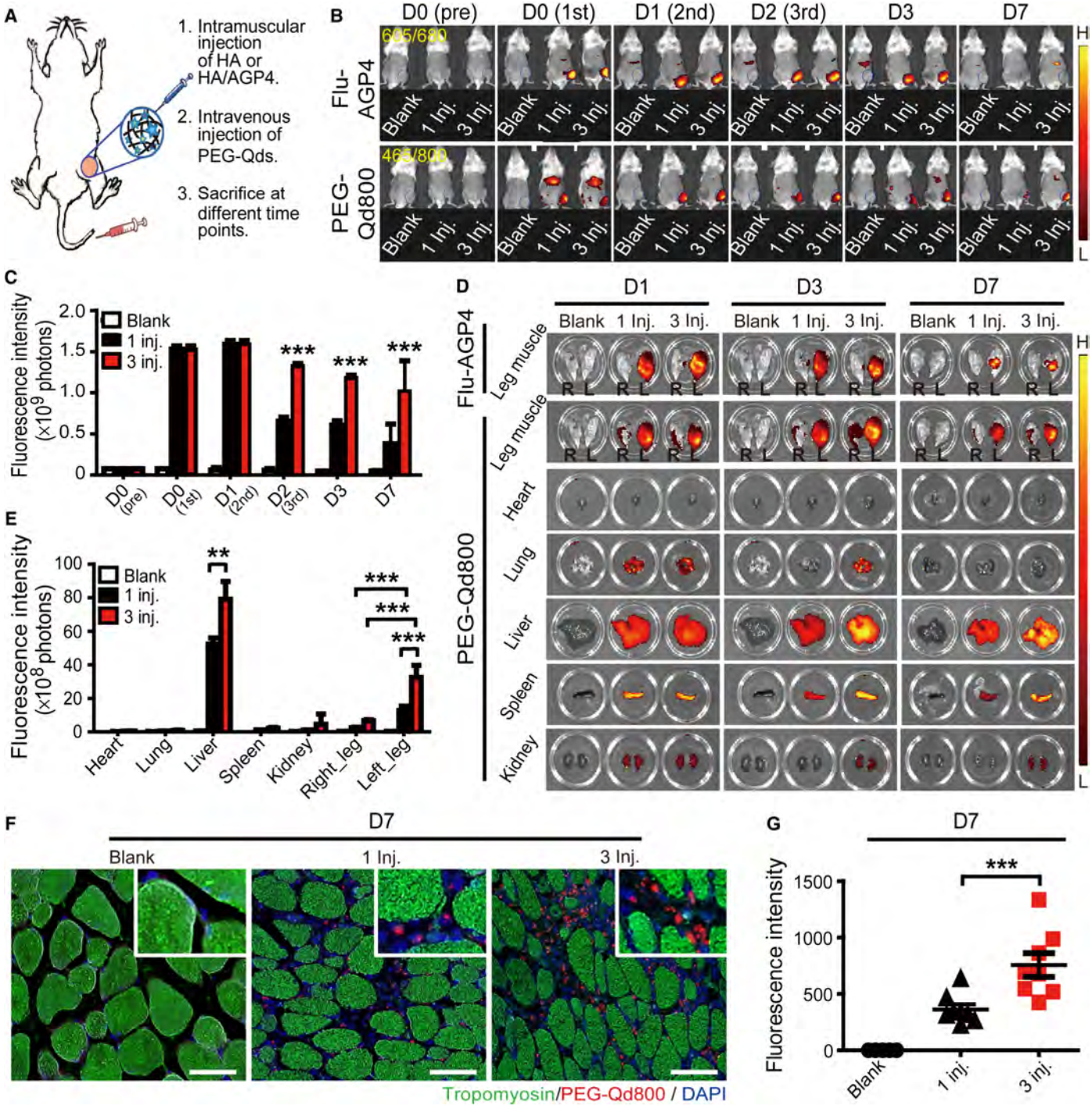

Fig. 2. In vivo demonstration of reloadable anti-PEG capture system. (**A**) Schematic diagram showing the experimental design. (**B**) Representative IVIS images of mice after one single intramuscular injection of Flu-AGP4 and first, second, and third intravenous administrations of PEG-Qd800s. (**C**) Quantification of PEG-Qd800 fluorescence intensity. (**D**) Representative IVIS images showing biodistribution of systemically injected PEG-Qd800s at days 1, 4, and 7 after either one or three administrations. HA/Flu-AGP4 was injected into the left (L) leg, and the right (R) leg served as a control (blank). (**E**) Quantification of PEG-Qd800 biodistribution. (**F**) Representative immunofluorescence images of mouse thigh muscle showing PEG-Qd800 retention at day 7 after either single systemic injection or three systemic injections of PEG-Qd800s. Green, tropomyosin; red, PEG-Qd800s. Scale bars, 20 μm; inset, ×2 magnification. DAPI, 4′,6-diamidino-2-phenylindole. (**G**) Quantification of PEG-Qd800 fluorescence intensity in immunofluorescence images. Data are means ± SD. Blank, $n = 3$; one injection, $n = 6$; three injections, $n = 6$.

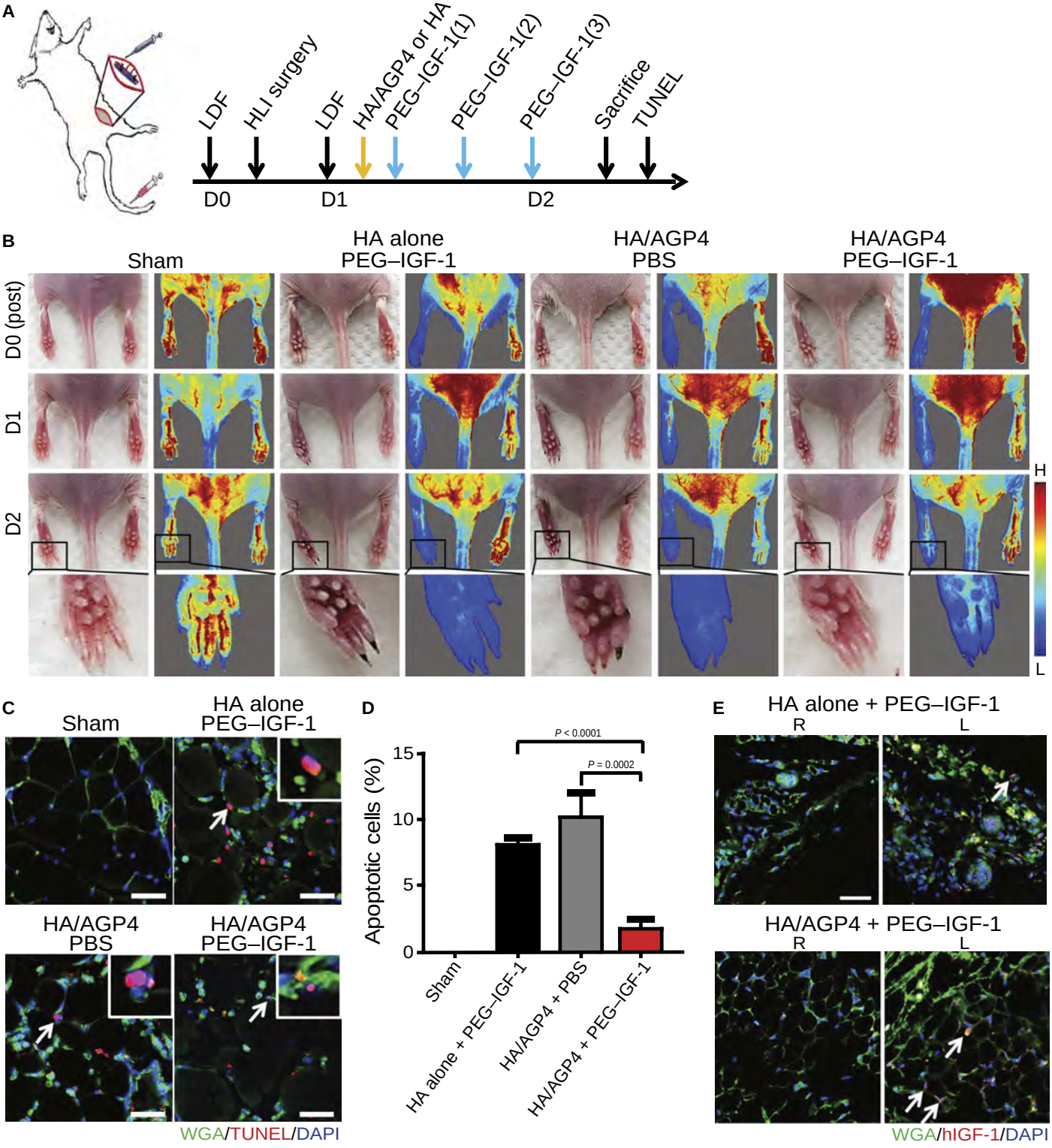

Fig. 3. Therapeutic efficacy of systemically injected PEG–IGF-1 combined with anti-PEG capture system. (**A**) Schematic diagram showing the experimental design. (**B**) Representative laser Doppler flowmetry (LDF) and photographs of mice after HLI in the left hind limb at days 0, 1, and 2. (**C**) TUNEL analysis of apoptotic cells (red) 2 days after treatment. Cell membranes were labeled with wheat germ agglutinin (WGA; green). Scale bars, 20 μm. (**D**) Quantification of apoptotic cell percentage according to TUNEL analysis. (**E**) Immunofluorescence staining for human IGF-1 (hIGF-1; red) and WGA (green). Scale bar, 50 μm. $n = 6$ for all groups.

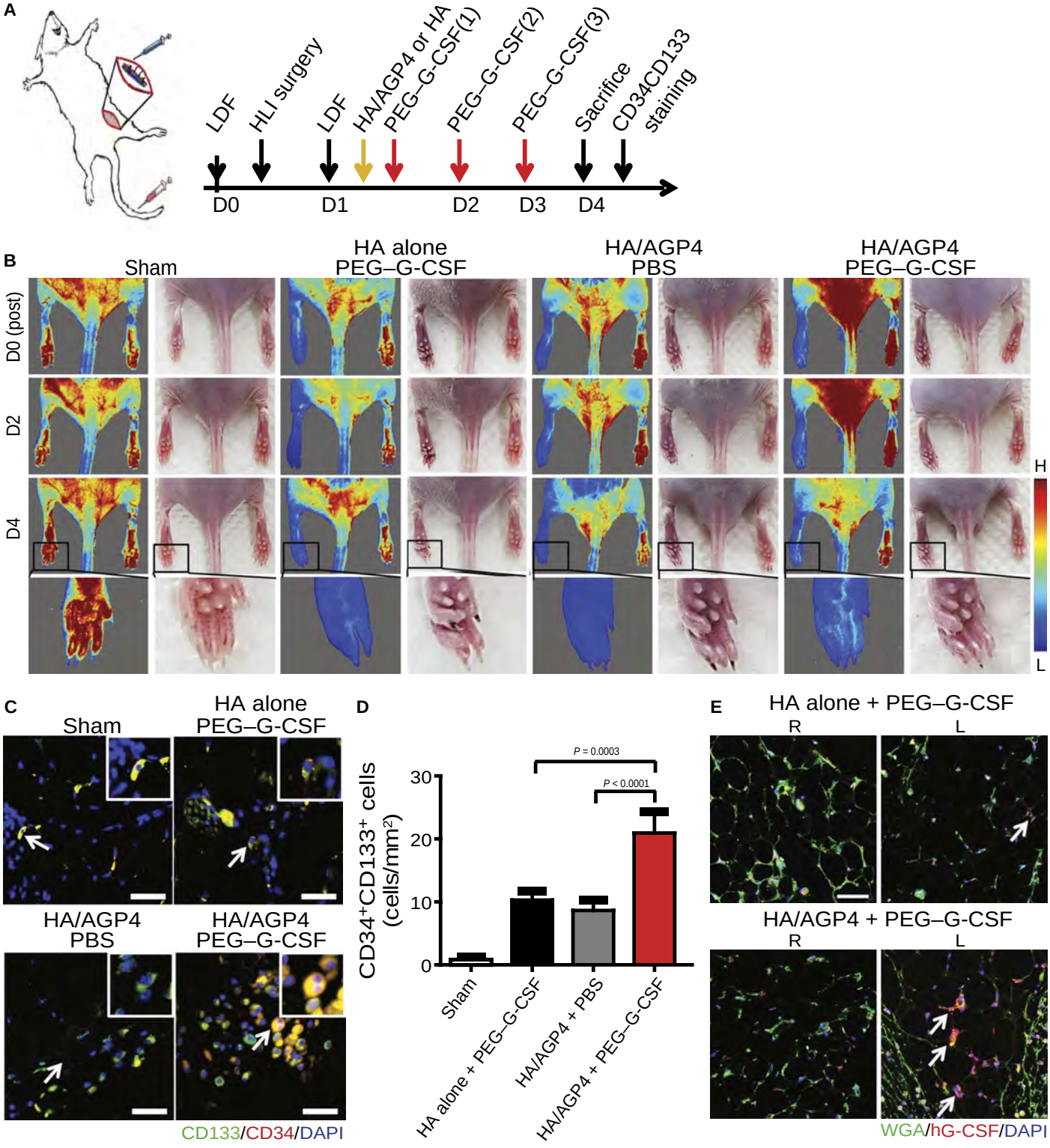

Fig. 4. Therapeutic efficacy of systemically injected PEG–G-CSF combined with anti-PEG capture system. (**A**) Schematic diagram showing the experimental design. (**B**) Representative LDF and photographs of mice after HLI in the left hind limb at days 0, 2, and 4. (**C**) Representative immunofluorescence images showing $CD133^+$ (green)/$CD34^+$ (red) progenitor cell recruitment at the intramuscular injection site. Scale bars, 20 μm. (**D**) Quantification of $CD133^+/CD34^+$ cell recruitment. (**E**) Immunofluorescence staining for human G-CSF (hG-CSF; red) and WGA (green). Scale bar, 50 μm. $n = 6$ for all groups.

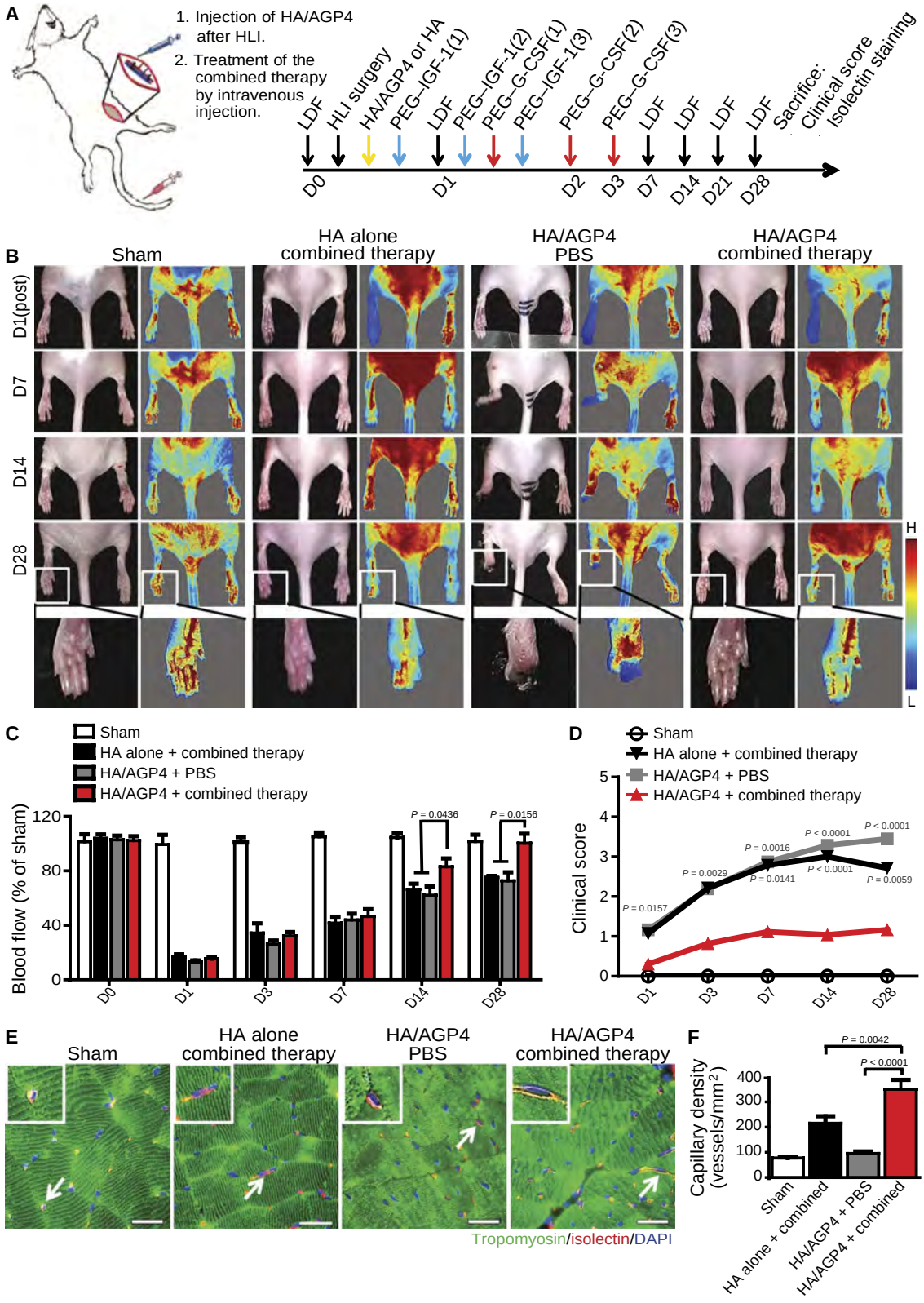

Fig. 5. Therapeutic efficacy of sequentially injected PEG–G-CSF and PEG–IGF-1 combined with anti-PEG capture system. (**A**) Schematic diagram showing the experimental design. (**B**) Representative LDF and photographs of mice after ischemia in the left hind limb at days 1, 7, 14, and 28. (**C**) Quantification of blood flow measured by LDF. (**D**) Clinical scores of mice after HLI. (**E**) Immunofluorescence staining of isolectin (red) and tropomyosin (green) in muscle tissue from hind limbs of mice receiving either PBS or combined therapy with HA alone or HA/AGP4. Scale bars, 20 μm. (**F**) Quantification of capillary density at the peri-injury region. Sham, $n = 8$; HA alone + combined therapy, $n = 8$; HA/AGP4 + PBS, $n = 12$; HA/AGP4 + combined therapy, $n = 12$.

functions (table S3), and histological examination of injected muscle tissue showed no increased infiltration of immune cells (fig. S4). Although a full-fledged investigation into potential immunogenicity or toxicity is beyond the scope of this current study, HA/AGP4 treatment appears safe and did not generate significant complement activation or infiltration of leukocytes into the injection site over the time course examined.

The HA/AGP4 capture system preserves its activity in a large-animal model of HLI

Two key challenges in the translation of therapies from the laboratory to the clinic are the unrepresentative injury models and unfeasible drug doses used in small animals. For example, mice have a high degree of collateral circulation, and our limb ischemia model was based on permanent ligation without reperfusion, thus affecting drug delivery to the affected area. Therefore, we sought to demonstrate the HA/AGP4 system in a porcine model of limb ischemia-reperfusion using adjusted, clinically relevant doses of HA/AGP4 and quantum dots.

To induce limb ischemia, the femoral artery was reversibly ligated at a location immediately distal to the bifurcation from the external iliac artery in both hind limbs for 3 hours, followed by reperfusion. A schematic timeline of this experiment is shown in Fig. 6A. A photograph of the animal shown in Fig. 6B indicates the occlusion site (marked by X) and the intramuscular injection sites for either HA/IgM or HA/AGP4. Successful reduction of blood flow upon occlusion and successful restoration of blood flow upon reperfusion were confirmed by laser Doppler, as shown in Fig. 6C. After restoration of blood flow, a skin flap was opened, and 1 ml of HA/IgM or HA/AGP4 was injected directly into the injured muscles. PEG-Qd800s (2 μM) were then administered by ear vein and allowed to circulate for 4 hours. The animal was sacrificed, and blood was aspirated before collection of five vital organs, HA/IgM, HA/AGP4-injected muscle, and a separate noninjected muscle site. A control muscle sample was collected from a different pig that did not receive quantum dot injection. Examination of the fluorescence signal by IVIS, shown in Fig. 6 (D and E), reveals increased retention of PEG-Qd800s in the HA/AGP4-injected muscle, and immunofluorescence staining, shown in Fig. 6F, confirms that the HA/AGP4 system could capture and retain systemically injected PEG-modified quantum dots in a large animal using greatly reduced doses of both antibody and quantum dots. Figure S5A shows the systemic biodistribution of quantum dots and the PEG-Qd800 signal present in the blood after systemic administration.

HA/AGP4 improves the efficacy of PEG–G-CSF therapy of limb ischemia in a large-animal model

An FDA-approved PEG-modified G-CSF (pegfilgrastim) was used as the model therapeutic in a porcine model of HLI. The binding affinity of pegfilgrastim with anti-PEG antibody was also examined by ELISA, and it was found to bind with high affinity (fig. S5B). IGF-1 was not used in this instance because there is no clinically available PEGylated variant obtainable. HLI was induced bilaterally in three pigs as described above, and successful occlusion and reperfusion were confirmed by laser Doppler (fig. S5, C and D). After successful reperfusion, a skin flap was opened and either HA/AGP4 or HA/IgM was injected into the injured muscle. Pegfilgrastim was then administered by ear vein at a dose of 4 μg/kg immediately afterward and then at 24 and 48 hours after surgery to reload the capture depots. The animals were sacrificed at 72 hours, and samples were collected as described above (Fig. 6G). CD34 and CD133 staining and quantification (Fig. 6, H and I) revealed a significant increase in progenitor cell recruitment in the HA/AGP4-treated limb compared to HA/IgM control (versus noninjected, $P = 0.0004$; versus HA/IgM, $P = 0.0016$; $n = 3$). In addition, increased human G-CSF at the injection site was detected by immunofluorescence staining (Fig. 6J) and Western blot (Fig. 6K). Complete blood count analysis before surgery and at 24, 48, and 72 hours after surgery confirmed the systemic action of PEG–G-CSF, as noted by a large increase in circulating white blood cells (table S4).

DISCUSSION

We have shown that a local capture depot consisting of HA hydrogel and anti-PEG IgM antibodies is capable of capturing and retaining a variety of PEG-modified compounds at a chosen target site. This approach was demonstrated in murine and porcine models and used to develop an effective treatment strategy for limb ischemia using PEG-modified IGF-1 and G-CSF. This treatment, in combination with the local capture depot, was more efficacious than injecting growth factors alone.

We believe that this capture system solves several of the problems associated with the delivery of PEG-modified therapeutics and creates numerous possibilities for more advanced, multidrug, multistep treatment strategies to be explored in the future. It is known that tissue protection and angiogenesis are precisely controlled, complex natural processes, and thus, it is expected that any treatment strategy should be similarly complex—using multiple compounds delivered in sequence over varying time points to accentuate the natural process.

PEGylation has been widely used to increase circulation time of drugs, prolonging systemic drug concentration and reducing the number of repeated injections necessary to achieve therapeutic effects (*24*). However, the modest EPR effect seen in ischemic tissues is insufficient at promoting the extravasation of PEGylated therapeutics into the targeted site (*25*, *26*).

One common approach to overcome this limitation is to preload peptide growth factors in a degradable hydrogel that is injected into the peri-infarct region, thus allowing sustained delivery of growth factors into the ischemia-injured tissue (*27*–*29*). However, this approach has serious limitations, namely, the poor spatiotemporal control of the therapeutic release, which is dictated entirely by the degradation rate of the gel. This simplistic approach only allows one single therapeutic delivery per local injection, and multiple growth factors would be released at the same rate, which may not be optimal for tissue protection and therapeutic angiogenesis. Several reports have shown the advantages and importance of combinatorial therapeutics in successful tissue regeneration (*30*–*32*). Many different approaches have been investigated to deliver a combination of drugs that target ischemic tissue (*33*, *34*). Specifically designed drug delivery vehicles have been engineered to precisely degrade and release drugs at a specific rate during active remodeling of ischemic tissue (*35*). However, these drug delivery systems have limited versatility. Once injected, the release profile is set, usually at about 24 to 48 hours, and cannot be adjusted. Furthermore, the choice of drugs has to be predetermined before injection.

Using a capture system coupled with intravenous therapeutic administration, as shown in this study, allows for multiple deliveries to one local injection site and allows for timed delivery of multiple therapeutics, such as IGF-1 immediately after injury to increase tissue protection and G-CSF over the following days to aid recruitment of hematopoietic progenitor cells.

There are several other expected benefits to this capture system–based approach. By enhancing the capture and retention of therapeutics

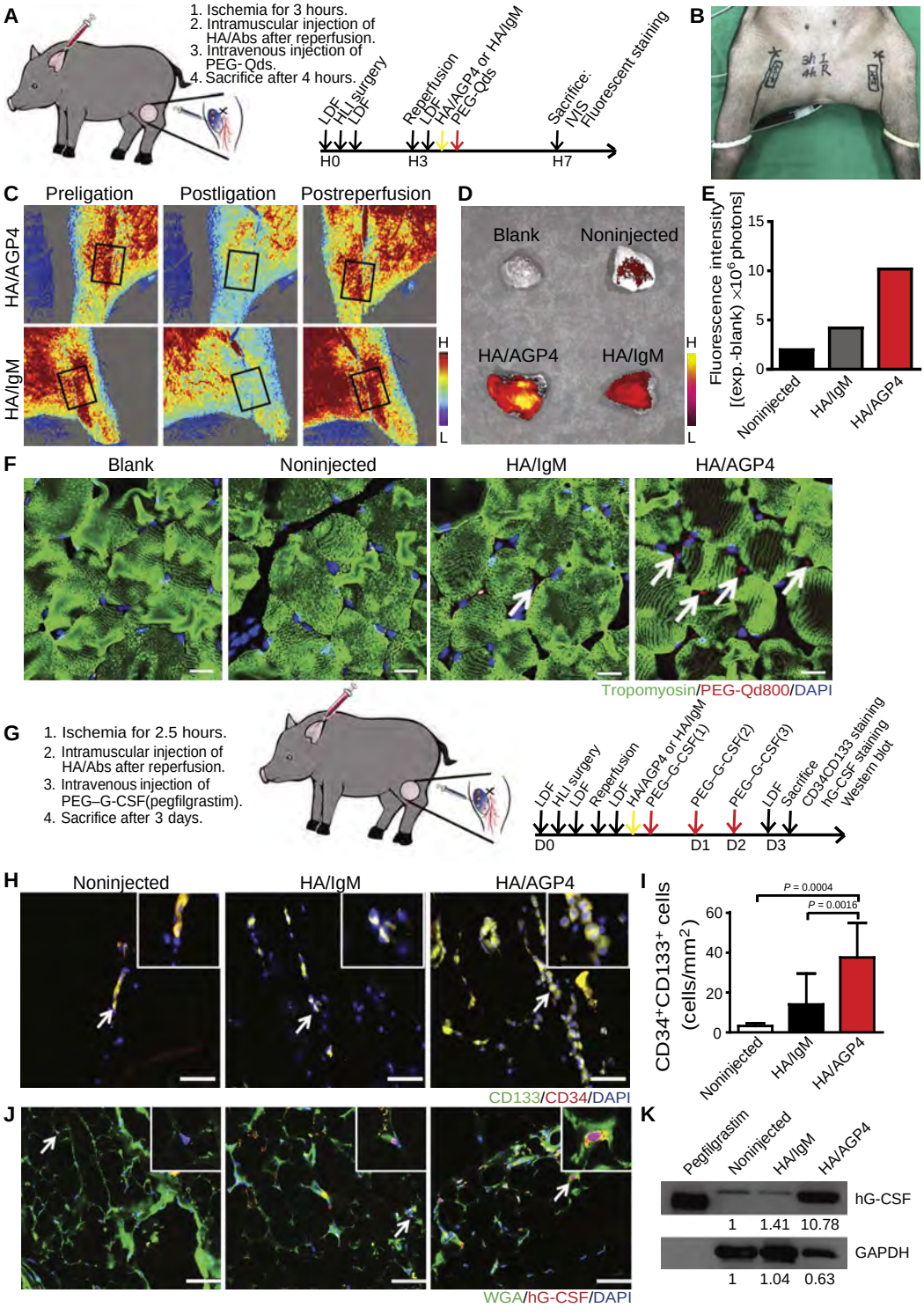

Fig. 6. Assessment of drug capture system in porcine model of hind limb ischemia-reperfusion. (**A**) Schematic diagram showing the experimental design of quantum dot capture experiment. Abs, antibodies. (**B**) Photograph showing location of artery occlusion (X) and HA-IgM or HA-AGP4 injection sites in both hind limbs. (**C**) LDF images of hind limb before ischemia, after ligation, and immediately after reperfusion. (**D**) Quantum dot analysis by IVIS of hind limb muscle tissue. A blank sample was obtained from a pig that did not receive quantum dot injection. The noninjected sample was from a portion of muscle tissue that did not receive hydrogel injection. (**E**) Quantification of quantum dot distribution by IVIS. (**F**) Immunofluorescence imaging of quantum dots (red) and tropomyosin (green) in hind limb samples. (**G**) Schematic diagram showing the experimental design of PEG–G-CSF (pegfilgrastim) therapy experiment. Scale bars, 20 μm. (**H**) Immunofluorescence staining of $CD133^+$ (green) and $CD34^+$ (red) cells 3 days after injury in ischemia-reperfusion–injured porcine muscle tissue. Scale bars, 20 μm. (**I**) Quantification of $CD133^+/CD34^+$ cell recruitment. (**J**) Human G-CSF (red) staining in ischemia-reperfusion–injured muscle tissue. Cell membranes were labeled with WGA (green). Scale bars, 50 μm. (**K**) Western blot analysis of human G-CSF isolated from ischemia-reperfusion–injured muscle tissue. Pegfilgrastim is shown as a positive control, and GAPDH (glyceraldehyde-3-phosphate dehydrogenase) is shown as a loading control. Quantum dots, $n = 2$; pegfilgrastim, $n = 3$.

at the injury site, this would facilitate the use of lower systemic doses of drugs. Similarly, because of the reloadable nature of the capture system, repeated lower systemic doses of therapeutic could be used to reach adequate local therapeutic concentrations, thus reducing side effects. In addition, improved targeting of PEG-modified compounds reduces their exposure to the host immune system (*36*, *37*). Studies have shown that sequential administration of PEGylated drugs may show progressively decreasing therapeutic efficacy because the surplus of the PEG moiety in plasma can induce a host immune response against PEG (*30*, *38*). Finally, this system allows for flexibility in a clinician's treatment regime, where timing and doses of multiple PEG-modified compounds can be adjusted in accordance with patient requirements and clinical progression. One reloadable depot system has been previously described (*39*), but this system relies on modifying existing drugs with custom-made complimentary oligodeoxynucleotides, which may affect drug pharmacokinetics and pharmacodynamics in unknown ways. We believe that the ability to capture PEGylated compounds is preferable, given the number of FDA-approved PEGylated therapeutics that are already on the market.

One weakness of this study is the relatively short time period examined, primarily because of the rapid degradation of HA hydrogel in vivo. We have shown that HA can retain the antibody at the local injection site for a maximum of 7 days, which may not be long enough for optimal treatment of some indications. However, for ischemia applications, it is preferential to administer therapy as soon as possible after injury. In addition, the clearance of intravenously administered growth factors, such as IGF-1, is typically measured in hours; thus, a 7-day capture window still allows time for multiple drug administrations, each one effectively "reloading" the local drug capture depot at the target site. Future studies will need to explore the use of more stable hydrogels to extend the duration of the capture system for use in other applications. Whereas HA hydrogel is generally accepted as safe and efficacious, the local IgM antibody carries the possibility of generating an immune response, although we did not detect this in our study.

Although application to limb ischemia is a suitable demonstration of this treatment strategy, we envisage that this approach would be most beneficial in other ischemic diseases, such as myocardial infarction or cerebrovascular ischemia, where multiple local injections into the ischemic site would be unfeasible. Furthermore, with an increasing number of PEG-modified therapeutics entering the market, we believe that this platform may also be extended to other applications in the future.

MATERIALS AND METHODS

Study design

The aim of this study was to examine whether an anti-PEG antibody–based drug capture system could improve the delivery and therapeutic efficacy of intravenously administered PEG-modified compounds. Murine and porcine experimental models of HLI were used, in accordance with approved protocols. Experimental groups received two component parts: a local injection of the drug capture system (HA hydrogel alone, HA with nonspecific IgM antibody as a control, or HA with IgM antibody specific against PEG) and the systemic injection of PEG-modified compounds, such as quantum dots or peptide growth factors. Sample sizes are indicated in figure legends throughout, and animals were randomly assigned to treatment groups after successful limb ischemia surgery. Experimentalists were blinded to the study groups when analyzing endpoints.

Experimental animals

All animal research protocols were approved by the Experimental Animal Committee of Academia Sinica, Taiwan. Mice (FVB/NJNarl, 8 to 10 weeks old) and pigs (Lanyu mini pigs, ~20 kg) were purchased from the National Laboratory Animal Center, Taiwan. Mice were anesthetized with xylazine (2 mg/kg; Bayer Healthcare) and tiletamine/zolazepam (50 mg/kg; Virbac) before surgery and in vivo measurements. Pigs were anesthetized with subcutaneous buprenorphine (0.05 mg/kg), intramuscular tiletamine/zolazepam (4 mg/kg) and xylazine (2.2 mg/kg), and subcutaneous atropine (0.05 mg/kg) and were intubated. Anesthesia was maintained by a mixture of oxygen, air, and isoflurane (1.5 to 2.0%). Heparin was given at 10 to 40 IU/kg. Saline, dextrose (glucose), and electrolytes were administered via an indwelling needle, which was placed in an ear vein, as deemed necessary during surgical procedures. Lidocaine (1%) spray was used for additional local anesthesia of the surgery site.

Sandwich ELISA

The protocol was described by Su *et al.* (*40*). Briefly, either AGP4 antibody or normal IgM (5 μg/ml) in 0.1 M $NaHCO_3/Na_2CO_3$ (pH 8.0) was coated onto a 96-well ELISA microplate for 4 hours at 37°C and then at 4°C overnight. Skim milk (2%) in PBS was used to block the plate for 2 hours at room temperature and then washed three times with PBS. PEG-Qd800 (Invitrogen), Lipo-Dox (TTY Biopharm), and PEG–G-CSF (pegfilgrastim, Amgen) diluted in 2% skim milk/PBS to different concentrations were incubated at room temperature for 2 hours. After washing, the plate was incubated with detection antibody 3.3-biotin (5 μg/ml) for 1 hour, followed by 1 hour with horseradish peroxidase–conjugated streptavidin (0.5 μg/ml) at room temperature. The plate was then incubated with 200 μl of ABTS solution [2,2′-azino-di(3-ethylbenzthiazoline-6-sulfonic acid) (0.4 mg/ml), 0.003% H_2O_2, and 100 mM phosphate citrate (pH 4.0)] in the dark for 15 min at room temperature. The absorbance at 405 nm was measured using a microplate reader.

Preparation of fluorescence-conjugated AGP4 and HA hydrogel

Alexa Fluor 647 (Invitrogen)–conjugated AGP4 was prepared according to the manufacturer's instructions. Gel chromatography was used to exclude the unbound antibody. The purified mixture was then centrifuged through 10-kDa MWCO Amicon Ultra centrifugal filter units (Millipore) to filter surplus Alexa Fluor 647 molecules. A 2% (w/v) HA/AGP4 hydrogel was formed by dissolving HA powder (1500 kDa; Creative PEGWorks) in sterile PBS or AGP4 (150 ± 10 μg)/PBS and agitated mildly at 4°C for 4 hours before use.

In vivo targeting profile and quantification

One day before the experiment, the mouse body was shaved and depilated using hair removal cream. Hydrogel mixtures were subcutaneously injected at three positions. Afterward, 30 μl of PEG-Qd800 (8 μM) was intravenously injected via lateral tail vein. For the analysis on sequential injections (Fig. 2), the hydrogel mixtures were injected into four chosen intramuscular sites. Then, a single injection of PEG-Qd800 was made on each site after 2 days. The noninvasive IVIS (PerkinElmer) was used to measure and localize the fluorescence signals of either fluorescence-labeled AGP4 or PEG-Qd800. The AGP4-injected sites were defined as the areas of region of interest (ROI) for quantification. At least three mice were measured for each treatment group, and the average results were subjected to statistical analysis. The same imaging

procedure and statistical analysis were performed on the extracted murine organs.

Intravital immunofluorescence imaging

The imaging procedure for the intravital multiphoton imaging experiment was conducted according to a previous publication (*41*). Before the experiment, the ears were depilated and wiped with 75% ethanol and water. All animals were anesthetized with 2.5% isoflurane (Minrad) and maintained in 1.5% isoflurane during the experiment. FITC-dextran mixed-HA hydrogel (HA-alone group) or HA/AGP4 hydrogel (HA/AGP4 group) was then intradermally injected into the left ear of each mouse. After stabilization for 4 hours, the labeled area was imaged by a multimode multiphoton scanning microscope, FVMPE-RS (Olympus). PEG-Qd655s (20 μl; Invitrogen) were injected by tail vein, and the labeled area was observed immediately afterward. The detected fluorescence signals were quantified by CellProfiler software, and the average was determined from three randomly chosen images.

Mouse HLI model and treatments

The surgical protocol of femoral artery ligation was performed as previously described (*42*). Briefly, HLI was induced by ligation, followed by the removal of left proximal femoral artery and distal femoral artery. The mice were then randomly divided into different treatment groups. One hundred microliters of 2% hydrogel of HA with or without AGP4 (150 ± 10 μg in total) was injected intramuscularly into four sites at the peri-ischemic area. For PEG–IGF-1 experiments, three doses of PEG–IGF-1 (1.5 mg/kg of body weight) were intravenously injected. The first injection was performed 2 hours after HA injection, with further doses given at 10 and 18 hours, for a total of three administrations. PEG–G-CSF (Creative Biomart) was intravenously injected 24 hours after HLI surgery, with further doses of PEG–G-CSF (50 μg/kg of body weight) given at 48 and 72 hours. For both experiments, mice were sacrificed on posttreatment day 2 or 4, and the distal calf and thigh muscles of both normal and ischemic legs were surgically removed, fixed overnight with 4% paraformaldehyde, and embedded for immunofluorescence staining, as previously described (*42*).

Apoptosis was determined by TUNEL assay (ApopTag Red In Situ Apoptosis Detection Kit, Millipore), and the assay was carried out according to the manufacturer's protocol. Cells recruited by PEG–G-CSF were confirmed by staining with anti-CD34 and anti-CD133 antibodies (Santa Cruz Biotechnology), as described below. The double-stained cells were quantified by ImageJ software.

Immunohistochemistry and immunofluorescence staining

Paraformaldehyde-fixed samples were embedded and boiled in sodium citrate (10 mM, pH 6.0) for 10 min, followed by staining with antibodies against CD34, CD133, tropomyosin, and isolectin (Invitrogen) at 4°C overnight, incubated with appropriate Alexa Fluor 488– or Alexa Fluor 568–conjugated secondary antibodies (Invitrogen), and then stained with 4′,6-diamidino-2-phenylindole. Capillary densities at the proximal ischemia zone were measured in eight randomly selected areas at a magnification of ×200 in each section by a blinded technician, and the values were averaged.

Blood flow measurement

An LDF device (Moor Instruments) was used to measure blood flow. Values for blood flow in both limbs were measured before the HLI surgery, immediately after the surgery, 1 day after surgery, and before sacrifice. In addition, for the combined protein experiment, blood flow was also recorded once a week for the following 4 weeks. Statistical analysis was performed on the blood flow at the ROI at the ischemic limb (left) compared to the normal limb (right). All LDF imaging and digital image capture of hind limb morphology were carried out by a blinded technician.

Clinical scoring of mice after HLI

Clinical scores were categorized into seven stages based on observation of mouse activity and hind limb appearance by a blinded expert. Clinical score criteria are described in detail in table S1.

Porcine HLI experiments

Limb ischemia was induced by reversible ligation of the femoral artery at a location immediately distal to the bifurcation from the external iliac artery in both hind limbs for 3 hours, followed by reperfusion. After reperfusion, a skin flap was opened, and 1 ml of hydrogel containing either 500 μg of AGP4 or IgM was injected across a designated area. PEG-Qd800s or pegfilgrastim (4 μg/kg) was administered by ear vein and allowed to circulate. Pigs were sacrificed, and blood was aspirated from the heart before sample collection.

C3 complement activation assay

HA hydrogel gel (30 μl) with 15 μg of antibody was injected locally into the left leg muscle at four sites. Plasma samples were taken before (day 0) and after injection (day 3). Mice were sacrificed on day 3, and muscle tissue was collected for analysis. Total protein concentration of plasma and muscle samples was determined by Pierce BCA (Thermo Fisher Scientific) assay. Samples and standards were added to the Mouse Complement C3 ELISA plate (Abcam) and incubated for 20 min at room temperature. Secondary detection antibodies were incubated for a further 20 min at room temperature before the absorbance was measured at 450 nm. Unknowns were determined using a standard curve. $n = 5$ per group.

Statistical analysis

Data are presented as means ± SD, unless otherwise indicated. The differences for multiple comparisons were analyzed by repeated-measures one-way analysis of variance (ANOVA) with Bonferroni adjustment. A P value of less than 0.05 was considered to represent statistical significance.

SUPPLEMENTARY MATERIALS

www.sciencetranslationalmedicine.org/cgi/content/full/8/365/365ra160/DC1
Fig. S1. Binding of anti-PEG antibody, AGP4, to PEGylated compounds.
Fig. S2. Characterization of fluorescently labeled AGP4 and PEG-Qd800.
Fig. S3. Schematic diagrams showing the setup for the intravital multiphoton microscopy experiment.
Fig. S4. Toxicity testing in immunocompetent mice.
Fig. S5. Supporting information for porcine HLI experiments.
Table S1. Clinical scoring system for murine limb ischemia morphology.
Table S2. White blood cell differential analysis in mice.
Table S3. Liver and kidney functions determined by serum biochemistry analysis in mice.
Table S4. White blood cell differential analysis in pigs after pegfilgrastim treatment.
Movie S1. Extravasation of systemically injected PEG-Qd655 in HA/AGP4-injected site.
Movie S2. Extravasation of systemically injected PEG-Qd655 in HA-alone–injected site.
Movie S3. Three-dimensional reconstructed images of PEG-Qd655 at HA/AGP4-injected site.
Movie S4. Three-dimensional reconstructed images of PEG-Qd655 at HA-alone–injected site.

REFERENCES AND NOTES

1. G. D. Yancopoulos, S. Davis, N. W. Gale, J. S. Rudge, S. J. Wiegand, J. Holash, Vascular-specific growth factors and blood vessel formation. *Nature* **407**, 242–248 (2000).

2. P. Carmeliet, Angiogenesis in health and disease. *Nat. Med.* **9**, 653–660 (2003).
3. S. E. Epstein, R. Kornowski, S. Fuchs, H. F. Dvorak, Angiogenesis therapy: Amidst the hype, the neglected potential for serious side effects. *Circulation* **104**, 115–119 (2001).
4. R. Cao, E. Bråkenhielm, R. Pawliuk, D. Wariaro, M. J. Post, E. Wahlberg, P. Leboulch, Y. Cao, Angiogenic synergism, vascular stability and improvement of hind-limb ischemia by a combination of PDGF-BB and FGF-2. *Nat. Med.* **9**, 604–613 (2003).
5. H. Zhang, Y. L. Yuan, Z. Wang, B. Jiang, C. S. Zhang, Q. Wang, X. H. Xu, H. Y. Dong, Z. M. Zhang, Sequential, timely and controlled expression of $hVEGF_{165}$ and Ang-1 effectively improves functional angiogenesis and cardiac function in vivo. *Gene Ther.* **20**, 893–900 (2013).
6. H. K. Awada, N. R. Johnson, Y. Wang, Sequential delivery of angiogenic growth factors improves revascularization and heart function after myocardial infarction. *J. Control. Release* **207**, 7–17 (2015).
7. W. Guan, A. Kozak, S. C. Fagan, Drug repurposing for vascular protection after acute ischemic stroke. *Acta Neurochir. Suppl.* **111**, 295–298 (2011).
8. S. Soliman, T. Ishrat, A. Y. Fouda, A. Patel, B. Pillai, S. C. Fagan, Sequential therapy with minocycline and candesartan improves long-term recovery after experimental stroke. *Transl. Stroke Res.* **6**, 309–322 (2015).
9. F. M. Chen, M. Zhang, Z. F. Wu, Toward delivery of multiple growth factors in tissue engineering. *Biomaterials* **31**, 6279–6308 (2010).
10. P. Bailon, A. Palleroni, C. A. Schaffer, C. L. Spence, W. J. Fung, J. E. Porter, G. K. Ehrlich, W. Pan, Z. X. Xu, M. W. Modi, A. Farid, W. Berthold, Rational design of a potent, long-lasting form of interferon: A 40 kDa branched polyethylene glycol-conjugated interferon α-2a for the treatment of hepatitis C. *Bioconjug. Chem.* **12**, 195–202 (2001).
11. H. Shibata, Y. Yoshioka, S. Ikemizu, K. Kobayashi, Y. Yamamoto, Y. Mukai, T. Okamoto, M. Taniai, M. Kawamura, Y. Abe, S. Nakagawa, T. Hayakawa, S. Nagata, Y. Yamagata, T. Mayumi, H. Kamada, Y. Tsutsumi, Functionalization of tumor necrosis factor-α using phage display technique and PEGylation improves its antitumor therapeutic window. *Clin. Cancer Res.* **10**, 8293–8300 (2004).
12. T. Ishida, K. Atobe, X. Wang, H. Kiwada, Accelerated blood clearance of PEGylated liposomes upon repeated injections: Effect of doxorubicin-encapsulation and high-dose first injection. *J. Control. Release* **115**, 251–258 (2006).
13. T. Ishida, M. Ichihara, X. Wang, K. Yamamoto, J. Kimura, E. Majima, H. Kiwada, Injection of PEGylated liposomes in rats elicits PEG-specific IgM, which is responsible for rapid elimination of a second dose of PEGylated liposomes. *J. Control. Release* **112**, 15–25 (2006).
14. E. Blanco, H. Shen, M. Ferrari, Principles of nanoparticle design for overcoming biological barriers to drug delivery. *Nat. Biotechnol.* **33**, 941–951 (2015).
15. M. Guvendiren, J. A. Burdick, Stiffening hydrogels to probe short- and long-term cellular responses to dynamic mechanics. *Nat. Commun.* **3**, 792 (2012).
16. B. P. Purcell, D. Lobb, M. B. Charati, S. M. Dorsey, R. J. Wade, K. N. Zellars, H. Doviak, S. Pettaway, C. B. Logdon, J. A. Shuman, P. D. Freels, J. H. Gorman III, R. C. Gorman, F. G. Spinale, J. A. Burdick, Injectable and bioresponsive hydrogels for on-demand matrix metalloproteinase inhibition. *Nat. Mater.* **13**, 653–661 (2014).
17. C. H. Chen, S. S. Wang, E. I. H. Wei, T. Y. Chu, P. C. H. Hsieh, Hyaluronan enhances bone marrow cell therapy for myocardial repair after infarction. *Mol. Ther.* **21**, 670–679 (2013).
18. E. D. Rabinovsky, R. D. Akli, Insulin-like growth factor I plasmid therapy promotes in vivo angiogenesis. *Mol. Ther.* **9**, 46–55 (2004).
19. E. Conti, C. Carrozza, E. Capoluongo, M. Volpe, F. Crea, C. Zuppi, F. Andreotti, Insulin-like growth factor-1 as a vascular protective factor. *Circulation* **110**, 2260–2265 (2004).
20. E. Yannaki, T. Papayannopoulou, E. Jonlin, F. Zervou, G. Karponi, A. Xagorari, P. Becker, N. Psatha, I. Batsis, P. Kaloyannidis, V. Tahynopoulou, V. Constantinou, A. Bouinta, K. Kotta, A. Athanassiadou, A. Anagnostopoulos, A. Fassas, G. Stamatoyannopoulos, Hematopoietic stem cell mobilization for gene therapy of adult patients with severe β-thalassemia: Results of clinical trials using G-CSF or Plerixafor in splenectomized and nonsplenectomized subjects. *Mol. Ther.* **20**, 230–238 (2012).
21. J. Honold, R. Lehmann, C. Heeschen, D. H. Walter, B. Assmus, K.-I. Sasaki, H. Martin, J. Haendeler, A. M. Zeiher, S. Dimmeler, Effects of granulocyte colony stimulating factor on functional activities of endothelial progenitor cells in patients with chronic ischemic heart disease. *Arterioscler. Thromb. Vasc. Biol.* **26**, 2238–2243 (2006).
22. M. D'Aveni, J. Rossignol, T. Coman, S. Sivakumaran, S. Henderson, T. Manzo, P. S. Sousa, J. Bruneau, G. Fouquet, F. Zavala, O. A. Prévot, M. G. Traoré, F. Suarez, H. T. Nègre, M. Mohty, C. L. Bennett, R. Chakraverty, O. Hermine, M. T. Rubio, G-CSF mobilizes $CD34^+$ regulatory monocytes that inhibit graft-versus-host disease. *Sci. Transl. Med.* **7**, 281ra42 (2015).
23. H. A. Himburg, G. G. Muramoto, P. Daher, S. K. Meadows, J. L. Russell, P. Doan, J.-T. Chi, A. B. Salter, W. E. Lento, T. Reya, N. J. Chao, J. P. Chute, Pleiotrophin regulates the expansion and regeneration of hematopoietic stem cells. *Nat. Med.* **16**, 475–482 (2010).
24. A. J. Murphy, S. Funt, D. Gorman, A. R. Tall, N. Wang, Pegylation of high-density lipoprotein decreases plasma clearance and enhances antiatherogenic activity. *Circ. Res.* **113**, e1–e9 (2013).
25. R. Kumar, I. Roy, T. Y. Ohulchanskky, L. A. Vathy, E. J. Bergey, M. Sajjad, P. N. Prasad, In vivo biodistribution and clearance studies using multimodal organically modified silica nanoparticles. *ACS Nano* **4**, 699–708 (2010).
26. H. Kobayashi, R. Watanabe, P. L. Choyke, Improving conventional enhanced permeability and retention (EPR) effects; what is the appropriate target? *Theranostics* **4**, 81–89 (2014).
27. J. R. Peña, J. R. Pinney, P. Ayala, T. A. Desai, P. H. Goldspink, Localized delivery of mechano-growth factor E-domain peptide via polymeric microstructures improves cardiac function following myocardial infarction. *Biomaterials* **46**, 26–34 (2015).
28. F. Chen, Q. Liu, Z. D. Zhang, X. H. Zhu, Co-delivery of G-CSF and EPO released from fibrin gel for therapeutic neovascularization in rat hindlimb ischemia model. *Microcirculation* **20**, 416–424 (2013).
29. R. S. Ripa, E. Jørgensen, Y. Wang, J. J. Thune, J. C. Nilsson, L. Søndergaard, H. E. Johnsen, L. Køber, P. Grande, J. Kastrup, Stem cell mobilization induced by subcutaneous granulocyte-colony stimulating factor to improve cardiac regeneration after acute ST-elevation myocardial infarction. Result of the double-blind, randomized, placebo-controlled stem cells in myocardial infarction (STEMMI) trial. *Circulation* **113**, 1983–1992 (2006).
30. Z. Tao, B. Chen, X. Tan, Y. Zhao, L. Wang, T. Zhu, K. Cao, Z. Yang, Y. W. Kan, H. Su, Coexpression of VEGF and angiopoietin-1 promotes angiogenesis and cardiomyocyte proliferation reduces apoptosis in porcine myocardial infarction (MI) heart. *Proc. Natl. Acad. Sci. U.S.A.* **108**, 2064–2069 (2011).
31. H. Lu, X. Xu, M. Zhang, R. Cao, E. Bråkenhielm, C. Li, H. Lin, G. Yao, H. Sun, L. Qi, M. Tang, H. Dai, Y. Zhang, R. Su, Y. Bi, Y. Zhang, Y. Cao, Combinatorial protein therapy of angiogenic and arteriogenic factors remarkably improves collaterogenesis and cardiac function in pigs. *Proc. Natl. Acad. Sci. U.S.A.* **104**, 12140–12145 (2007).
32. G. Kibria, H. Hatakeyama, N. Ohga, K. Hida, H. Harashima, Dual-ligand modification of PEGylated liposomes shows better cell selectivity and efficient gene delivery. *J. Control. Release* **153**, 141–148 (2011).
33. P. H. Kim, H. G. Yim, Y. J. Choi, B. J. Kang, J. Kim, S. M. Kwon, B.-S. Kim, N. S. Hwang, J. Y. Cho, Injectable multifunctional microgel encapsulating outgrowth endothelial cells and growth factors for enhanced neovascularization. *J. Control. Release* **187**, 1–13 (2014).
34. S. H. Shin, J. Lee, K. S. Lim, T. Rhim, S. K. Lee, Y. H. Kim, K. Y. Lee, Sequential delivery of TAT-HSP27 and VEGF using microsphere/hydrogel hybrid systems for therapeutic angiogenesis. *J. Control. Release* **166**, 38–45 (2013).
35. A. S. Salimath, E. A. Phelps, A. V. Boopathy, P. Che, M. Brown, A. J. García, M. E. Davis, Dual delivery of hepatocyte and vascular endothelial growth factors via a protease-degradable hydrogel improves cardiac function in rats. *PLOS ONE* **7**, e50980 (2012).
36. A. A. Bhirde, B. V. Chikkaveeraiah, A. Srivatsan, G. Niu, A. J. Jin, A. Kapoor, Z. Wang, S. Patel, V. Patel, A. M. Gorbach, R. D. Leapman, J. S. Gutkind, A. R. H. Walker, X. Chen, Targeted therapeutic nanotubes influence the viscoelasticity of cancer cells to overcome drug resistance. *ACS Nano* **8**, 4177–4189 (2014).
37. X. Wang, T. Ishida, H. Kiwada, Anti-PEG IgM elicited by injection of liposomes is involved in the enhanced blood clearance of a subsequent dose of PEGylated liposomes. *J. Control. Release* **119**, 236–244 (2007).
38. C. Borselli, H. Storrie, F. Benesch-Lee, D. Shvartsman, C. Cezar, J. W. Lichtman, H. H. Vandenburgh, D. J. Mooney, Functional muscle regeneration with combined delivery of angiogenesis and myogenesis factors. *Proc. Natl. Acad. Sci. U.S.A.* **107**, 3287–3292 (2010).
39. Y. Brudno, E. A. Silva, C. J. Kearney, S. A. Lewin, A. Miller, K. D. Martinick, M. Aizenberg, D. J. Mooney, Refilling drug delivery depots through the blood. *Proc. Natl. Acad. Sci. U.S.A.* **111**, 12722–12727 (2014).
40. Y. C. Su, B. M. Chen, K. H. Chuang, T. L. Cheng, S. R. Roffler, Sensitive quantification of PEGylated compounds by second-generation anti-poly(ethylene glycol) monoclonal antibodies. *Bioconjug. Chem.* **21**, 1264–1270 (2010).
41. J. L. Li, C. C. Goh, J. L. Keeble, J. S. Qin, B. Roediger, R. Jain, Y. Wang, W. K. Chew, W. Weninger, L. G. Ng, Intravital multiphoton imaging of immune responses in the mouse ear skin. *Nat. Protoc.* **7**, 221–234 (2012).
42. A. Limbourg, T. Korff, L. C. Napp, W. Schaper, H. Drexler, F. P. Limbourg, Evaluation of postnatal arteriogenesis and angiogenesis in a mouse model of hind-limb ischemia. *Nat. Protoc.* **4**, 1737–1748 (2009).

Acknowledgments: We acknowledge R. H. Lin and Y. P. Wong for assistance in animal surgery; B. M. Chen and Y. C. Su [Institute of Biomedical Sciences (IBMS), Academia Sinica] for help with antibody affinity assays; and R. Liao (Brigham and Women's Hospital, Boston, MA), M. E. Davis (Emory University and Georgia Institute of Technology, Atlanta, GA), and R.-B. Yang (IBMS, Academia Sinica, Taipei) for helpful discussions. **Funding:** This work was supported by the National Research Program

for Biopharmaceuticals of the Ministry of Science and Technology (MOST 102-2321-B-001-069 and 104-2325-B-001-010) and the Ministry of Health and Welfare (104TM1001), the Academia Sinica Translational Medicine Program, and the Academia Sinica Nanoscience and Nanotechnology Program, Taiwan. **Author contributions:** P.C.H.H. initiated the idea; J.P.J.W., S.R.R., and P.C.H.H. designed the experiments; J.P.J.W., B.C., D.J.L., C.Y.T.Y., S.R.R., P.C., and P.C.H.H. performed the experiments and analyzed the data; J.J.L., S.H.P., and P.S.S. provided critical comments on the study; and J.P.J.W., B.C., D.J. L., and P.C.H.H. wrote the manuscript. **Competing interests:** P.C.H.H., J.P.J.W., B.C., and S.R.R. are co-inventors on a pending patent application for the use of HA and AGP4 for cardiovascular therapy. The other authors declare that they have no competing interests.

Submitted 25 November 2015
Resubmitted 22 July 2016
Accepted 1 October 2016
Published 16 November 2016
10.1126/scitranslmed.aah6228

Citation: J. P. J. Wu, B. Cheng, S. R. Roffler, D. J. Lundy, C. Y. T. Yen, P. Chen, J. J. Lai, S. H. Pun, P. S. Stayton, P. C. H. Hsieh, Reloadable multidrug capturing delivery system for targeted ischemic disease treatment. *Sci. Transl. Med.* **8**, 365ra160 (2016).

Science Translational Medicine
AAAS

Reloadable multidrug capturing delivery system for targeted ischemic disease treatment

Jasmine P. J. Wu, Bill Cheng, Steve R. Roffler, David J. Lundy, Christopher Y. T. Yen, Peilin Chen, James J. Lai, Suzie H. Pun, Patrick S. Stayton and Patrick C. H. Hsieh (November 16, 2016)
Science Translational Medicine **8** (365), 365ra160. [doi: 10.1126/scitranslmed.aah6228]

Editor's Summary

Free refills on ischemia treatment

Restoring functional tissue after ischemia is thought to require neovascularization to replace the occluded blood vessels. Neovascularization can be induced by growth factor proteins, but they generally have short half-lives in circulation and are difficult to deliver to the site of injury. Wu *et al*. have designed a reloadable system that uses antibodies embedded in a hydrogel to capture tagged growth factor therapeutics and retain them at the site of ischemic injury. Moreover, it can be easily reloaded by intravenous injection of additional growth factors doses, which are then captured by the antibody-based system. The authors demonstrated the efficacy and safety of this system in mouse and pig models of limb ischemia, suggesting a potential for future clinical development.

Science Translational Medicine (print ISSN 1946-6234; online ISSN 1946-6242) is published weekly, except the last week in December, by the American Association for the Advancement of Science, 1200 New York Avenue, NW, Washington, DC 20005.

Science Translational Medicine
AAAS

www.sciencetranslationalmedicine.org/cgi/content/full/8/365/365ra160/DC1

Supplementary Materials for

Reloadable multidrug capturing delivery system for targeted ischemic disease treatment

Jasmine P. J. Wu, Bill Cheng, Steve R. Roffler*, David J. Lundy, Christopher Y. T. Yen, Peilin Chen, James J. Lai, Suzie H. Pun, Patrick S. Stayton, Patrick C. H. Hsieh*

*Corresponding author. Email: phsieh@ibms.sinica.edu.tw (P.C.H.H.); sroff@ibms.sinica.edu.tw (S.R.R.)

Published 16 November 2016, *Sci. Transl. Med.* **8**, 365ra160 (2016)
DOI: 10.1126/scitranslmed.aah6228

The PDF file includes:

Other Supplementary Material for this manuscript includes the following:
(available at www.sciencetranslationalmedicine.org/cgi/content/full/8/365/365ra160/DC1)

Movie S4 (.avi format). Three-dimensional reconstructed images of PEG-Qd655 at HA-alone–injected site.

Figure S1

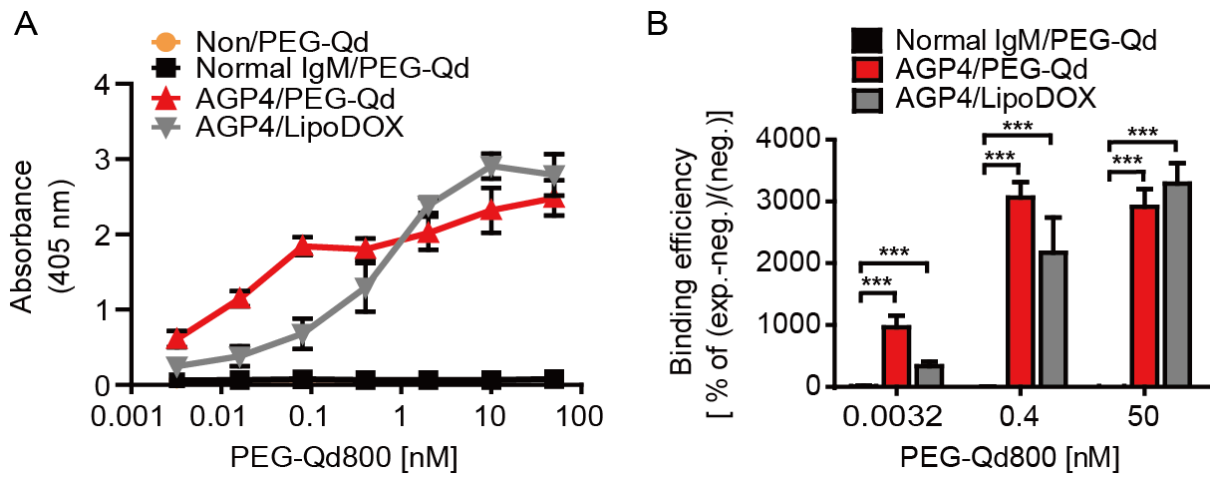

Figure S1. Binding of anti-PEG antibody, AGP4, to PEGylated compounds.

(A) The binding profile of PEGylated compounds to wells coated with AGP4 antibodies. (B) The binding efficiency of PEG-Qd800 to AGP4 in comparison to its binding to IgM, and the binding of LipoDOX to AGP4. The data are presented as mean ± s.d.. (***P < 0.001 vs. normal IgM/PEG-Qd-treated).

Figure S2

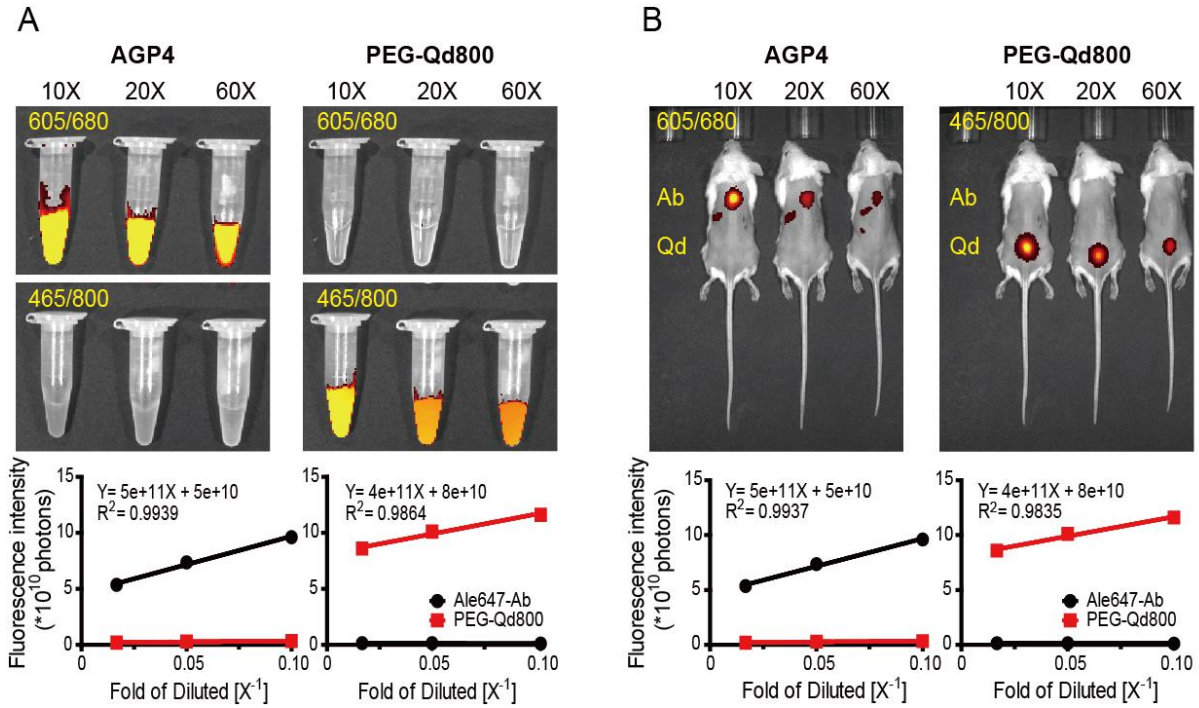

Figure S2. Characterization of fluorescently labeled AGP4 and PEG-Qd800.

The emission signals of Alexa 647 dye-labelled AGP4 and PEG-Qd800 at different dilutions, under the excitation 605 nm (AGP4, Ab) and 465 nm (PEG-Qd800, Qd) in vitro (A) and in vivo (B).

Figure S3

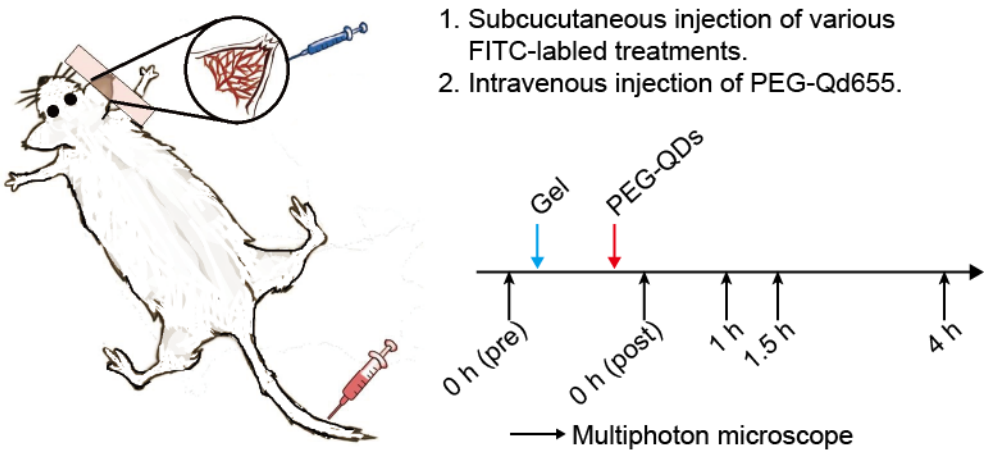

Figure S3. Schematic diagrams showing the setup for the intravital multiphoton microscopy experiment.

Figure S4

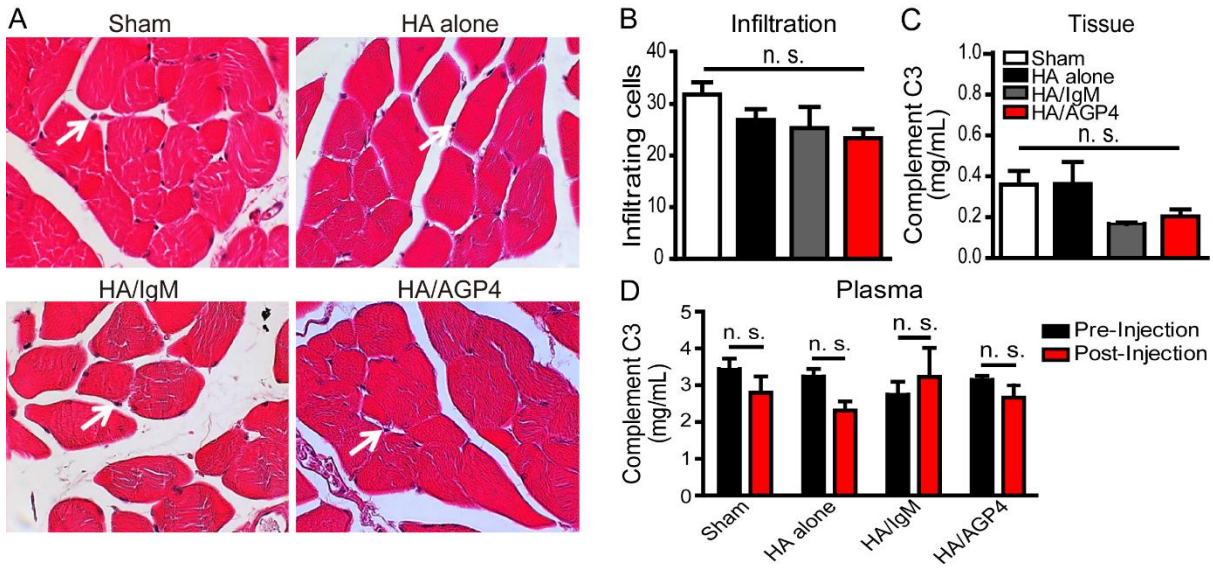

Figure S4. Toxicity testing in immunocompetent mice.

(A) H&E stained muscle tissue showing immune cell infiltration (examples shown by white arrows). (B) Quantification of immune cell infiltration (n = 5 per group). (C) C3 complement activation 3 days after injection at local injection site. (D) C3 complement activation in plasma before and 3 days after local injection in each treatment group. n = 5 per group. n.s; no significant difference ($P > 0.05$).

Figure S5

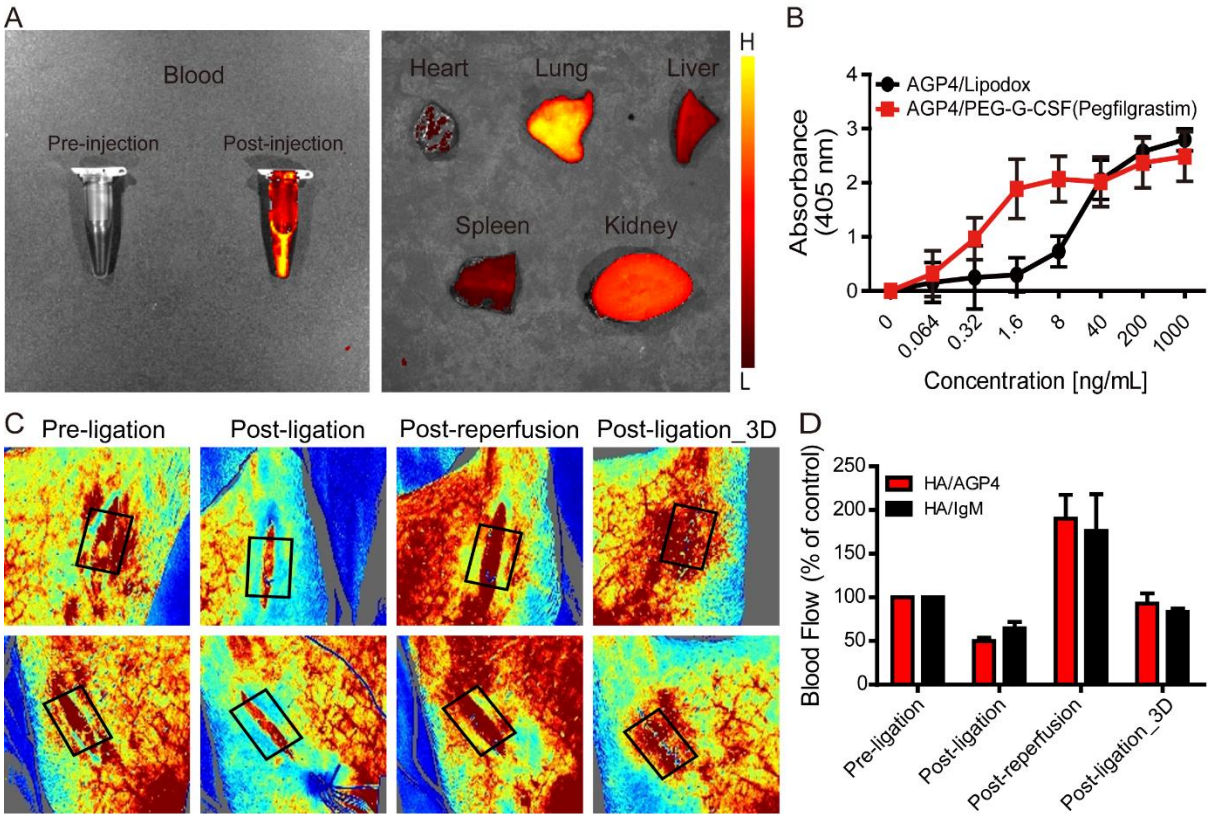

Figure S5. Supporting information for porcine HLI experiments.

(A) Left: IVIS image showing blood sample taken before and after PEG-Qd800 systemic administration; right: PEG-Qd800 retention in 5 vital organs. (B) ELISA assay showing binding affinity of AGP4 anti-PEG IgM antibody and pegfilgrastim used in these experiments. (C) Sample laser Doppler flowmetry images showing blood flow before, during, after, and 3 days after reversible limb ischemia in pigs. The region of interest is shown as a black box around the skin flap which was opened to facilitate HA/antibody injection. (D) Graph showing average blood flow change compared to pre-occlusion baseline. No significant difference was found between the groups. n = 3 pigs for pegfilgrastim experiments.

Table S1. Clinical scoring system for murine limb ischemia morphology.

Clinical Score System:	
0	Normal
1	Gait abnormality with muscle dystrophy
2	Moderate discoloration with muscle atrophy (> 2 nails)
3	Severe discoloration with muscle atrophy (> 2 toes)
4	Toe necrosis (4.5+ loss of toe* 0.1)
5	Foot necrosis or gangrene
6	Limb amputation

Table S2. White blood cell differential analysis in mice.

Murine	Sham		HA alone		HA/IgM		HA/AGP4		
	D0	D3	D0	D3	D0	D3	D0	D3	Ref.
WBC (K/μL)	6.45±1.85	3.18±1.48	7.17±1.65	2.26±1.17	6.76±1.17	2.64±1.33	7.36±1.59	3.09±1.88	9.3±1.6
NEU (%)	19.16±3.9	38.44±12.7	19.52±5.4	40.58±15.7	16.4±2.2	41.2±12.9	21.68±2.1	51.1±11.5	12.1±5.0
LYM (%)	76.76±5.0	57.76±13.9	77.48±6.1	51.68±22.2	80.02±2.8	53.53±15.9	73.34±3.3	42.76±12.0	83.7±4.7
MONO (%)	0.58±0.3	1.12±1.0	0.4±0.2	0.42±0.4	0.48±0.1	1.675±1.9	0.48±0.2	0.34±0.5	3.0±1.81
EOS (%)	3.36±2.0	2.64±2.0	2.6±1.1	6.46±6.9	3.04±1.3	3.25±3.5	4.3±1.7	5.8±2.7	2.97±1.25

WBC: white blood cells; NEU: neutrophils; LYM: lymphocytes; MONO: monocytes; EOS: eosinophils. Ref. is the normal reference range.

Table S3. Liver and kidney functions determined by serum biochemistry analysis in mice.

Murine	Sham		HA alone		HA/IgM		HA/AGP4		
	D0	D3	D0	D3	D0	D3	D0	D3	Ref.
GOT (U/l)	90.2± 33.8	99.25 ±28.4	59.4 ±4.04	75.5 ±10.8	64.25 ±20.0	74.33 ±6.3	63.2 ±6.91	91.6 ±21.9	100.2 ±22
GPT (U/l)	34.2 ±5.97	34.25 ±4.3	43±4.2	40.5 ±4.5	40.25 ±2.63	32.67 ±5.9	36.4 ±4.77	33.8 ±6.4	37.0 ±14.1
BUN (mg/dl)	20.5 ±1.97	21.38 ±5.2	18.68 ±2.15	20.45 ±0.6	23±2.92	20.75 ±1.6	21.56 ±2.18	15.78 ±1.0	30.2 ±4.71
CRE (mg/dl)	0.12 ±0.04	0.32 ±0.04	0.14 ±0.05	0.28 ±0.05	0.15 ±0.06	0.28 ±0.05	0.2±0	0.26 ±0.05	0.26 ±0.05

GOT: Glutamic-Oxaloacetic Transaminase (AST); GPT: Glutamic-Pyruvic Transaminase (ALT); BUN: blood urea nitrogen; CRE: creatinine.

Table S4. White blood cell differential analysis in pigs after pegfilgrastim treatment.

Porcine	CBC				
	D0	D1	D2	D3	Ref.
WBC (K/μL)	12.59±5.83	23.78±6.08	29.65±0.69	23.79±3.63	11-22
NEU (%)	41.99±5.83	63.58±9.21	66.62±4.99	59.39±4.08	28-51
LYM (%)	51±7.94	30.6±7.08	27.05±4.10	35.57±5.11	39-62
MONO (%)	1.3±0.28	0.78±0.168	1.08±0.36	1.44±0.27	2-10
EOS (%)	4.74±2.16	4.64±2.28	4.75±1.78	3.38±1.05	0.5-11

WBC: white blood cells; NEU: neutrophils; LYM: lymphocytes; MONO: monocytes; EOS: eosinophils.

Movie S1. Extravasation of systemically injected PEG-Qd655 in HA/AGP4-injected site.

Movie S2. Extravasation of systemically injected PEG-Qd655 in HA-alone–injected site.

Movie S3. Three-dimensional reconstructed images of PEG-Qd655 at HA/AGP4-injected site.

Movie S4. Three-dimensional reconstructed images of PEG-Qd655 at HA-alone–injected site.